Characterization of Lunar Dust for Toxicological Studies. II: Texture and Shape Characteristics

Yang Liu[1]; Jaesung Park[2]; Darren Schnare[3]; Eddy Hill[4]; and Lawrence A. Taylor[5]

Abstract: The morphology (shape and texture) of dust fractions of five Apollo lunar soils and a lunar dust simulant, JSC-1Avf, was studied using scanning electron microscopy. Shape (aspect ratio and complexity) of particles was described based on the two-dimensional projection images. The distributions of aspect ratio and complexity of particles are reported. It was determined that the Apollo lunar dust particles consist mainly of impact-produced glass, with complicated morphologies, extensive surface areas per grain, and sharp, jagged edges. Importantly, many grains contain elaborate vesicular textures, representing minute agglutinates. Dust simulant JSC-1Avf also has similar shapes as lunar dust, but differs in surface texture and area (smooth and nonvesicular). These data provide information for toxicity studies of lunar dust and for selecting a suitable lunar dust simulant.

DOI: 10.1061/(ASCE)0893-1321(2008)21:4(272)

CE Database subject headings: Dust; Moon; Toxicity; Morphology.

Introduction

Recently, NASA announced its plan for returning humans to the Moon and establishing a lunar base in the next two decades, and then to move on to Mars, and beyond. For this purpose, tapping into the resources in the lunar regolith presents great benefits over transportation of materials from Earth. However, prior to establishment of any robotic or manned plant for the in situ resource utilization (ISRU) required for long-duration operations, the problem of lunar dust must be seriously addressed and mitigated (Taylor et al. 2005). The deleterious nature of lunar dust (<20 μm fraction) became apparent with the first Apollo mission, but was tolerated rather than mitigated because of the rapid succession of short missions. Importantly, lunar dust (brought in by the dirty spacesuits) contaminated the atmosphere in the lunar module and irritated astronauts' eyes, sinuses, and throats (e.g., Apollo 12, 17 Technical Crew Debriefings). In contrast to short exposure during the Apollo missions, astronauts in the future Moon base might be subject to prolonged exposure if the presence of lunar dust is not substantially mitigated.

Lunar regolith was produced in a unique environment. With the absence of an effective atmosphere (133×10^{-6} Pa), the surface of the Moon has been continuously bombarded by meteorites and micrometeorites that produced the lunar regolith through the comminution of rock and minerals. However, many of these same micrometeorites (<1 mm) have sufficient kinetic energy to melt small fractions of the lunar soil. The impact-generated melt quenches to aggregate rock and mineral particles to form agglutinates (McKay et al. 1991). At the same time, the hypervelocity of the impact can vaporize portions of the melt, which is then deposited as glass coatings with abundant nanophase metallic iron (Keller and McKay 1993; 1997; Wentworth et al. 1999). The abundance of the impact-generated glass with nanophase-Fe^0 (np-Fe^0) increases with decreasing grain size to ~80% at <10 μm (Taylor et al. 2001). Therefore, the <1 μm fraction of lunar dust consists almost entirely of impact glass, mostly with np-Fe^0.

It has been suggested that the <2.5 μm fraction of terrestrial dust particles may be correlated with adverse cardiovascular diseases (Delfino et al. 2005, and references cited therein). It is suggested that the ultrafine particles (<0.1 μm) can be translocated directly into blood circulation and cause damage to different organs (Delfino et al. 2005; Gwinn and Vallyathan 2006; Nemmar et al. 2002). Tests on carbon nanoparticles (Mills et al. 2006) showed that a small amount of the ultrafine particles (<0.1 μm) may translocate directly into the systemic circulation and to target organs. Although the gravity on the Moon is only 1/6th that of Earth's, the deposition of particles of a few micrometers in the lung is similar or higher than those on Earth (Darquene et al. 1997, 1998, 1999). Therefore, the possible link between nano-sized lunar dust and human health needs to be addressed.

Previous toxicity studies on lunar soil by Holland and Simmonds (1973) and Kustov et al. (1989) produced indecisive results. Lam et al. (2002a,b) studied the toxicity of the dust of lunar soil simulant (JSC-1) and Martian soil simulant, TiO_2, and SiO_2 on rats. They found that a single, high-dose of simulants can cause acute responses and chronic effects after 90 days. However, because lunar dust bears numerous np-Fe^0, the terrestrial simulant did not fully mimic the toxicity of lunar dust. Particle sizes and shapes are important factors for toxicity studies (Guthrie 1997). It is imperative that detailed information on the morphology (shape

[1]Postdoctoral Research Associate, Planetary Geosciences Institute, Dept. of Earth and Planetary Sciences, Univ. of Tennessee, Knoxville, TN 37996. E-mail: yangl@utk.edu

[2]Research Associate, Planetary Geosciences Institute, Dept. of Earth and Planetary Sciences, Univ. of Tennessee, Knoxville, TN 37996.

[3]Research Specialist, Planetary Geosciences Institute, Dept. of Earth and Planetary Sciences, Univ. of Tennessee, Knoxville, TN 37996.

[4]Research Associate, Planetary Geosciences Institute, Dept. of Earth and Planetary Sciences, Univ. of Tennessee, Knoxville, TN 37996.

[5]Professor, Planetary Geosciences Institute, Dept. of Earth and Planetary Sciences, Univ. of Tennessee, Knoxville, TN 37996.

Note. Discussion open until March 1, 2009. Separate discussions must be submitted for individual papers. The manuscript for this paper was submitted for review and possible publication on September 14, 2006; approved on December 6, 2006. This paper is part of the ***Journal of Aerospace Engineering***, Vol. 21, No. 4, October 1, 2008. ©ASCE, ISSN 0893-1321/2008/4-272–279/$25.00.

and surface texture) and particle-size distribution of lunar dust particles be obtained for dust-mitigation purposes and for toxicity studies (James 2005). Given the lack of availability of Apollo lunar samples for ISRU studies, lunar soil simulants are widely used for testing purposes. However, choice of a suitable simulant is only possible after we have determined the morphological features of lunar dust.

Morphological studies of lunar soil were mainly conducted in 1970s. Except for two studies (Görz et al. 1971, 1972), most of the previous studies on the surface texture of Apollo soil samples have been focused on grains larger than the defined dust size (i.e., >20 μm) (e.g., Carter and MacGregor 1970; Cloud et al. 1970; Fruland et al. 1977; Heywood 1971; McKay et al. 1970, 1973; Mueller 1971). These studies show that the surface of soil fragments is commonly coated with splashed glass produced by melting during meteorite impacts. This glass presents textures ranging from coherent frothy coatings to dispersed glass mounds. Görz et al. (1971, 1972) analyzed shapes and sizes of lunar soil grains down to 1.25 μm, using a scanning electron microscope. Liu et al. (2006) reported the unique vesicular grains found in Apollo 17 dust. In line with the study of particle size distribution (Park et al. 2008, 2006a,b), the morphology (texture and shape) of dust samples (<20 μm) is presented here for samples studied in Park et al. (2008) (Apollo soil 10084, 70051, and lunar dust simulant, JSC-1Avf), as well as three additional lunar soil samples (Apollo 12001, 15041, 79221).

Sample Selection and Methods

Apollo samples 10084 and 70051 are lunar soils that have been dry sieved to be <1 mm at the Johnson Space Center and were then dry sieved to the <43 μm fraction in our lab. The other three lunar soil samples were used in previous studies and wet sieved to <10 μm (Noble et al. 2001; Taylor et al. 2001). JSC-1Avf is the fine fraction (<20 μm) of a new production of former lunar simulant JSC-1, which was initially chosen in 1993 to approximate the geotechnical properties of the average lunar soil (Klosky et al. 1996). JSC-1A and JSC-1 are made from the same basaltic tuff, and have relatively high glass contents (~50%; McKay et al. 1994; Hill et al. 2007).

The sample preparation method used in this study is similar to that in Park et al. (2008) and is briefly summarized below. To a representative small portion (<5 mg) of each sample, ~5 mL of a surfactant solution was added (poly-*N*-vinylpyrrolidone in isopropanol). This mixture was sonicated for 10–30 min to separate attached particles. It was determined that this mild sonication was sufficient to disassociate the smaller particles from the surfaces of the larger ones, yet this does not change the grain size measurably. The isopropanol solution of poly-*N*-vinylpyrrolidone can efficiently separate particles, comparing Fig. 1(j) with other images in Fig. 1. A small amount (~3 μL) of the mixture was then taken with a micropipette, dropped on a cleaned silicon wafer placed above a strong Nd-magnet to keep particles from clumping. This technique ensures that the long axis of the particle is nearly parallel to the silicon plate, which enables the study of largest surface area.

Literally hundreds of digital images of the samples, at two different magnifications (1,000× and 5,000× or 6,000×), were taken with a JOEL LSM-6060LV scanning electron microscope (SEM). The spatial resolution is 0.1 μm/pixel at 1,000×, 0.020 μm/pixel at 5,000×, and 0.016 μm at 6,000×. Because the z direction in SEM images cannot be calibrated, photographs of the particles were considered as two-dimensional (2D) projections. Areas and perimeters of the 2D digital photographs of the particles were measured directly by ImageJ software (http://rsb.info.nih.gov/ij/) [Fig. 1(a)]. The circular-equivalent diameter was calculated using the measured area.

Parameters characterizing particle shapes needed to be selected. Many shape factors have been suggested in the literature (e.g., Barrett 1980; Alshibli and Alsaleh 2004; Bouwman et al. 2004). However, factors for describing three-dimensional (3D) images or surface roughness cannot be used here. Because of the 2D nature of SEM images, we select two simple factors: "aspect ratio" and "complexity factor," in order to compare with Görz et al. (1971, 1972). For each particle, ImageJ least-squares fits an ellipse to the measured area [Fig. 2(a)]. In Görz et al. (1971, 1972), the ellipse was least-squares fit to the measured perimeter. With the fitted ellipse, aspect ratio and complexity factor were used to characterize the shape of particles (Fig. 2). The aspect ratio, a measure of elongation, is defined as the (minor axis)/(major axis) of the fitted ellipse [Fig. 2(a)]. The complexity factor, a measure of angularity of the particle, is the ratio of the measured perimeter to the calculated ellipse perimeter. Fig. 2(b) shows the aspect ratio and complexity factor for several geometrical shapes. The fitted-ellipse approximates well the real elongation of different shapes. Although the aspect ratio may be the same, the complexity factor can increase with increasing angularity or irregularity of the shape. A large number (1,200–7,200) of lunar particles were analyzed to provide statistically sound distribution curves.

Morphology of Lunar Samples

Particle Types

Based on SEM images of hundreds of particles, as well as those reported in literature (e.g., McKay et al. 1991, and references there in) lunar dust grains can be classified into the following five types:

Glass Beads. [For example, Figs. 1(a–c and e)]. These beads are volcanic beads, or shock-melt, produced during micrometeorite impacts, that has quenched in flight. Geometrical shapes of glass beads are diverse from perfect round spheres [Fig. 1(b)] to elongated ellipsoids [Fig. 1(c)], dumbbells [Fig. 1(a)], and teardrops [e.g., Fig. 1(e)] as the centrifugal forces increase (Fulchignoni et al. 1971). The ejected melt can possess a rotating momentum such that the torque and the centrifugal force competing with the surface tension can stretch the melt into shapes other than spherical. Glass beads are quite common, and are found in all size ranges. Except for some broken teardrops [Fig. 1(e)], glass beads are smooth and rounded.

Vesicular Texture. [For example, Figs. 1(h–k)]. Grains with this texture contain vesicles of different sizes (diameter: 0.1–4 μm) in a glassy matrix. These vesicles are formed by the solar-wind volatiles escaping during the melting from the micrometeorite impacts, thereby producing agglutinates. This texture occurs on all scales in glass grains or in glass coatings of other grains [e.g., Figs. 1(e, f, m, and n)]. Vesicular fragments >10 μm [Figs. 1(i–k)] are rarely found in the samples studied. These large vesicular grains may contain interior bubbles as

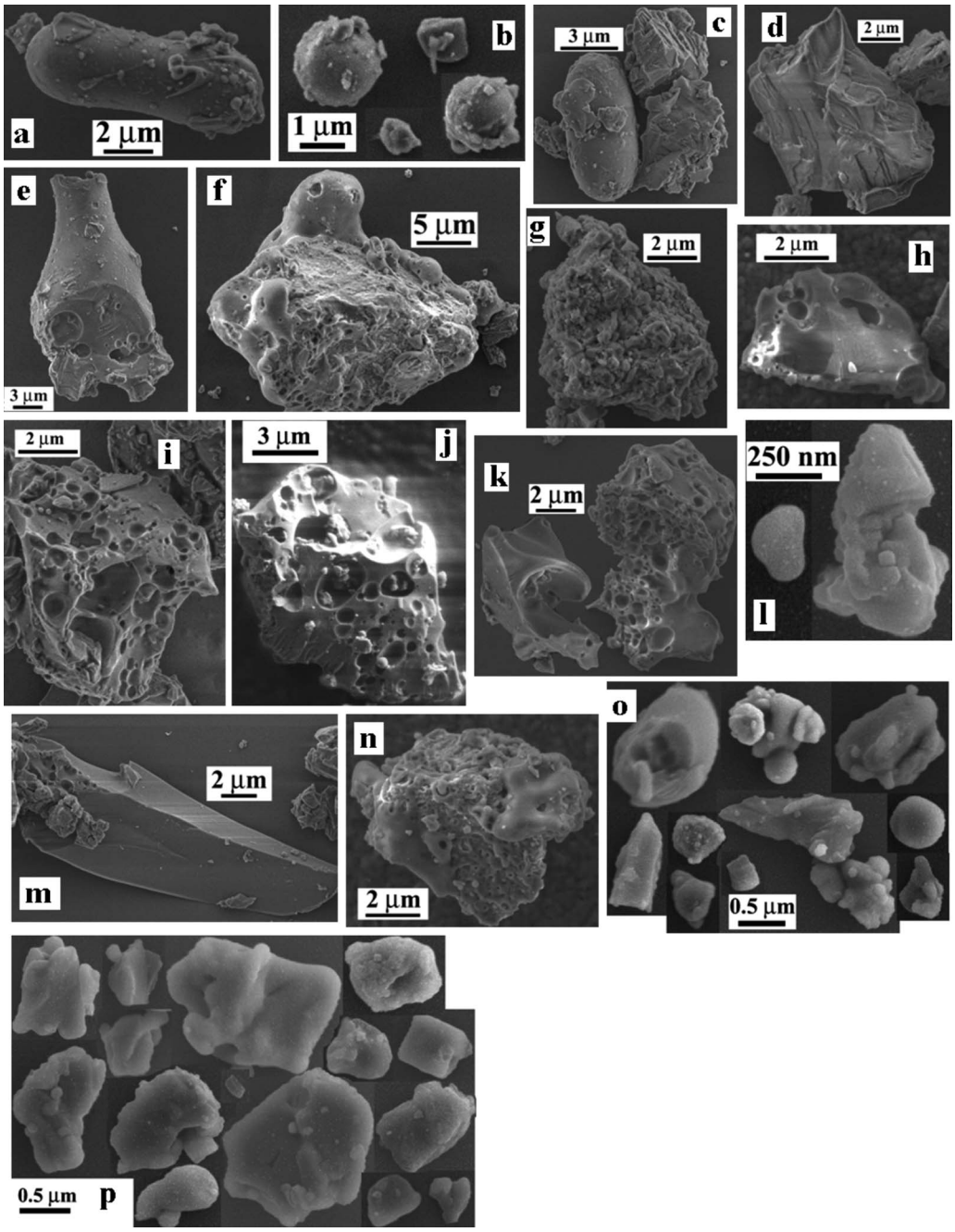

Fig. 1. Representative SEM images of lunar dust particles. Particles in all images except (*j*) were cleaned with the surfactant solution. (Adapted from Liu et al. 2006.)

shown by the holes on the vesicle wall. Smaller fragments with remnant vesicle walls are commonly observed. Broken vesicles result in grains with sharp edges and jagged shapes. The presence of high concentrations of submicron bubbles in this texture results in large reaction-surface areas (see discussion to follow).

Angular Shards. [For example, , Figs. 1(m and o)]. Angular shards are typically broken glasses with sharp edges as a result of crushing of larger glassy fragments. These shards have relatively smaller aspect ratios [down to 0.12 in Fig. 1(m)] than other particle types (dumbbells, ~0.2–0.3). The long axis of angular shards is generally greater than 10 μm. Angular shards with large aspect ratio (~1) are seen in grains <1 μm.

Blocky Fragments. [For example, , Figs. 1(c and d)]. These grains are broken mineral and rock grains. Broken minerals tend to have irregular edges, some due to cleavages (oriented structural weaknesses) in the minerals [Fig. 1(c)]. Such grains are in the distinct minority in these dust samples.

Aggregated Particles. [For example, , Fig. 1(g)]. This type of texture includes small particles loosely attached to each other or to the surface of large particles [Fig. 1(g)]. This texture is normally found on uncleaned samples.

Except for glass beads and some blocky fragments, most lunar dust grains have jagged edges. The first three types are typical for impact-generated glass and are commonly found in all particle

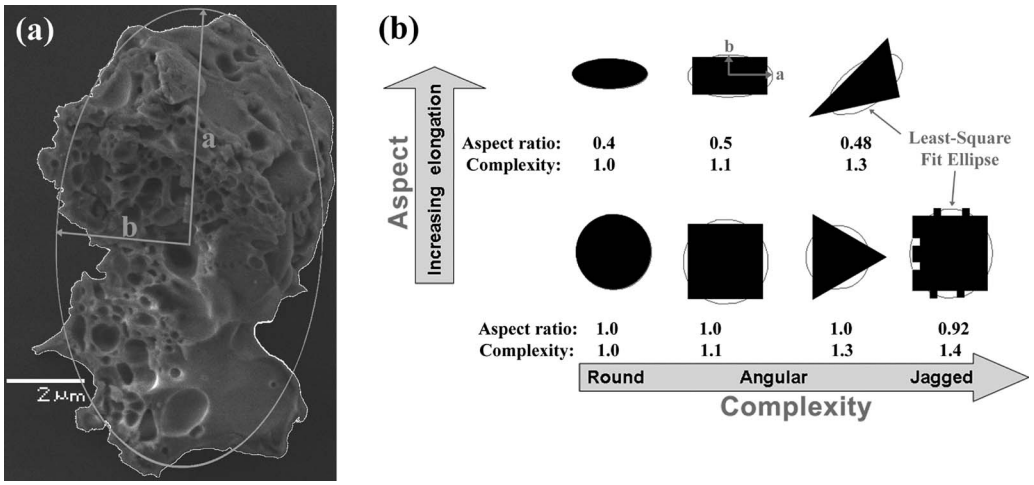

Fig. 2. Shape characterization. (a) Example of shape determination. White curve outline the perimeter (P) of the particle and the ellipse is the least-squares fit to the measured area. The major and minor axes are $2a$ and $2b$, respectively. The aspect ratio (ar) is the ratio of $2b/2a$ and the complexity is the ratio of measured perimeter over the calculated one of the fitted ellipse. (b) Variation of aspect ratio and complexity of several geometrical shapes. The fitted ellipses are in gray color.

sizes, which is consistent with the fact that the fine fractions of lunar soil are enriched in a glass component (Taylor et al. 2001), up to >80%. The first three types are of great importance because it is the impact-produced glass that contains the ubiquitous nanophase metallic Fe grains (Keller and McKay 1993, 1997; Wentworth et al. 1999).

The surfaces of most particles have different degrees of glass coating [e.g., lesser extent in Figs. 1(e and m); more pronounced in Figs. 1(f and n)]. Coatings form lobes or mounds [Figs. 1(f and n)] that act to increase the surface area of the particle (see discussion to follow). Fig. 1(f) shows a good example of a melt coating on an otherwise blocky grain, which altered the particle shape from smooth rounded to irregular jagged.

Shape Distributions of Lunar Dust Grains

For each sample, 1,200–7,200 particles were measured. The data are separated into two size categories (>1 μm and <1 μm) using the circular-equivalent diameter. Shape parameters for the >1 μm particles are from images at 1,000×, and those for <1 μm particles are from images at 5,000× and 6,000× magnifications. This is the first report of particle shapes for lunar dust particles <1 μm.

- ***Aspect ratios:*** Distributions of aspect ratios of all five lunar samples show a peak at ~0.7 (Fig. 3). Grains >1 μm and <1 μm have similar distributions, except for the <1 μm grains of 12001 and 15041, with more broad distributions. All distribution curves, however, are skewed toward a small aspect ratio. About 3–12% (in numbers) of particles have an aspect ratio <0.4. Görz et al. (1971, 1972) determined the aspect ratio of 55–300 particles >2 μm by least-squares fit to the measured perimeters. Although the detailed fit methods are different, the aspect ratios are still comparable. Our results are similar to the results of six Apollo 14 and 15 soils by Görz et al. (1972), but larger than that (0.53–0.62) of one Apollo 12 soil by Görz et al. (1971). The differences for the Apollo 12 soils may be that Görz et al. (1971) only measured grains with circular-equivalent diameter of 3.19–6.12 μm.
- ***Complexity factors:*** Complexities for all five lunar samples center at ~1.15 (Fig. 4), suggesting an angular shape [Fig. 2(b)]. These distribution curves skew toward complexity factors >1.25, indicating a significant proportion of angular and jagged grains. The complexity factors are slightly larger for more mature samples (1.2–1.3 for 79221, 1.2 for 15041) than those of submature (1.1–1.2 for 10084) or unmature samples (1.1–1.2 for 12001). As mentioned earlier, Görz et al. (1972) conducted least-squares fit to the measured diameter, and thus their complexity factors are always close to 1. Therefore, our complexity factors are not directly comparable to those reported in Görz et al. (1972).

Surface Areas of Lunar Dust Grains

Compared to a volume-equivalent solid particle, the surface area of individual vesicular particles is greatly increased by the presence of vesciles. Because of the irregular shape of the particle and vesicles, and the lack of information on the depth in SEM images, images of vesicular particles were considered as 2D slices of a 3D particle. Therefore, the surface area is transformed to the perimeter and the volume to cross-sectional area. Using this assumption, the increase of perimeter and cross-sectional area due to vesicles of several vesicular grains are shown in Fig. 5. Total perimeters of vesicular particles increase by a factor of 2–5 compared to the equal-volume, vesicle-free grains. For grains with similar vesicular contents, the surface areas can be quite different depending on the total number of vesicles present.

The mounds and folds of glass coatings on the surface of grains also contribute to increase the surface area of particles. For example, for a cube of 1 μm edge, attachment of 10 small cubes of 0.1 μm edge on each surface can increase the total surface area by a factor of 1.4.

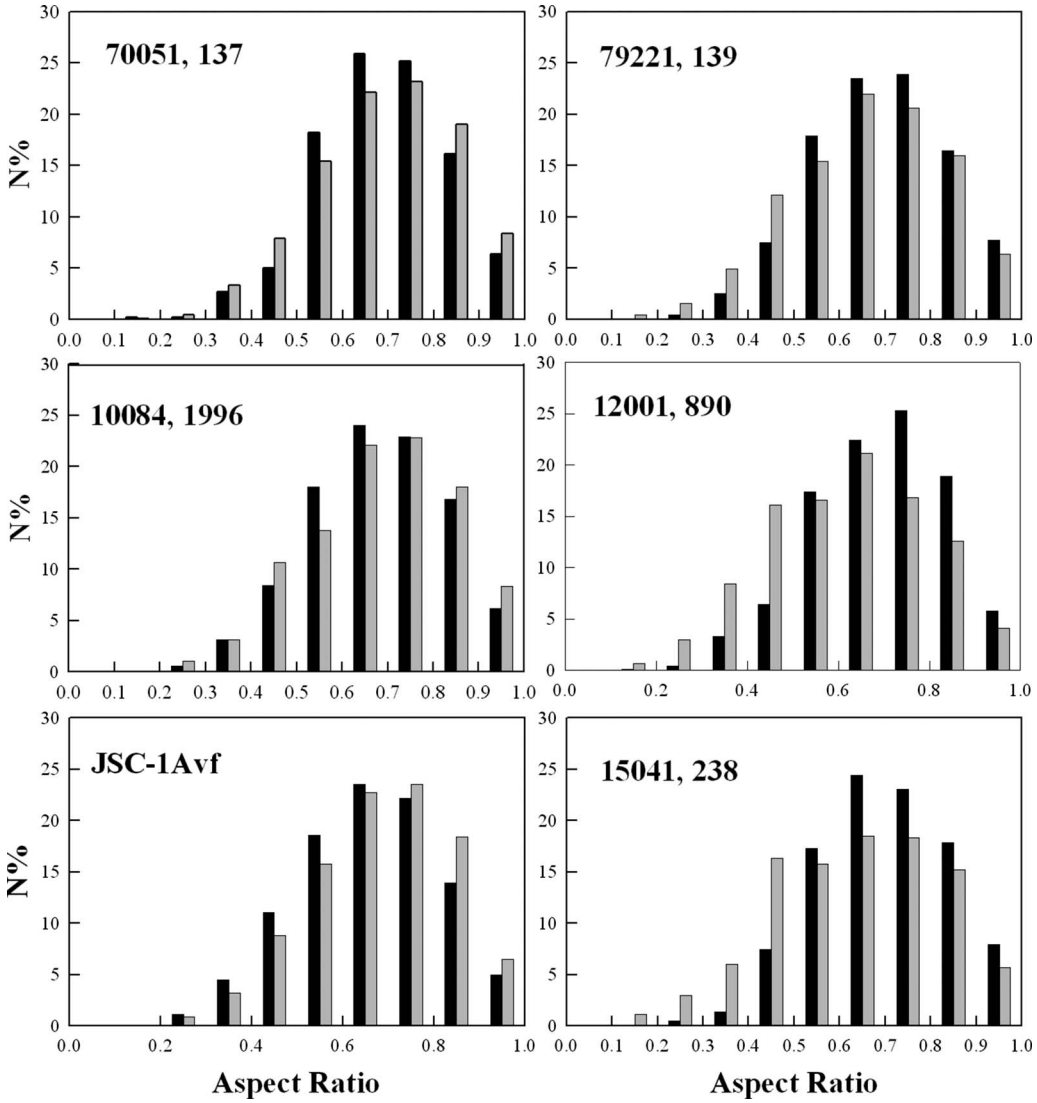

Fig. 3. Aspect ratios of five lunar soils and a simulant JSC-1Avf

Morphology of Simulant JSC-1Avf

Simulant JSC-1Avf consists mainly of blocky, angular, and acicular grains (Fig. 6). Some blocky grains have a rough surface [Figs. 6(f) and one in Fig. 6(g)], whereas most grains have a smooth surface. Sharp edges are also common. For particles <1 μm, blocky grains are the most abundant. Aspect ratios of the <1 μm and >1 μm fractions of JSC-1Avf are similar and have a peak of about 0.7. The complexity distribution of the <1 μm and >1 μm fractions of JSC-1Avf centers at 1.1–1.2.

Discussion

Comparison of Lunar Dust and Simulant JSC-1Avf

The surface areas of dust grains are greatly increased by high abundance of small particles. Park et al. (2008, 2006a) reported that 50% of the dust particles of Apollo 11 sample 10084 and Apollo 17 sample 70051 are <0.1 and 0.3 μm, respectively, but 50% of JSC-1Avf is <0.6 μm. Considering equivalent masses and making the assumption that particles are smooth spheres. For example, on the basis of surface area per unit mass, the total surface area for particles with 0.1 μm diameter is two orders of magnitude larger than that with 1 μm diameter. Therefore, the two lunar samples, 10084 and 70051, contain relatively larger total surface areas than the JSC-1Avf simulant. However, a detailed distribution function is required to derive an accurate calculation of surface area.

The aspect ratios of JSC-1Avf are similar to those of lunar soils. The complexity factor of >1 μm JSC-1Avf is similar to those of lunar soils. But for the <1 μm particles, JSC-1Avf has a narrower distribution in complexity than the real lunar samples (Fig. 4). Overall, the shape of JSC-1Avf is comparable to that of lunar dust. However, there are many differences between lunar dust and JSC-1Avf. First, simulant JSC-1Avf particles contain smoother outlines (Fig. 6) than those of lunar dust particles (Fig. 1), because simulant JSC-1Avf was prepared by mechanical crushing and grinding. The distribution of complexity factors of JSC-1Avf is narrower than lunar soils (Fig. 4). Second, simulant

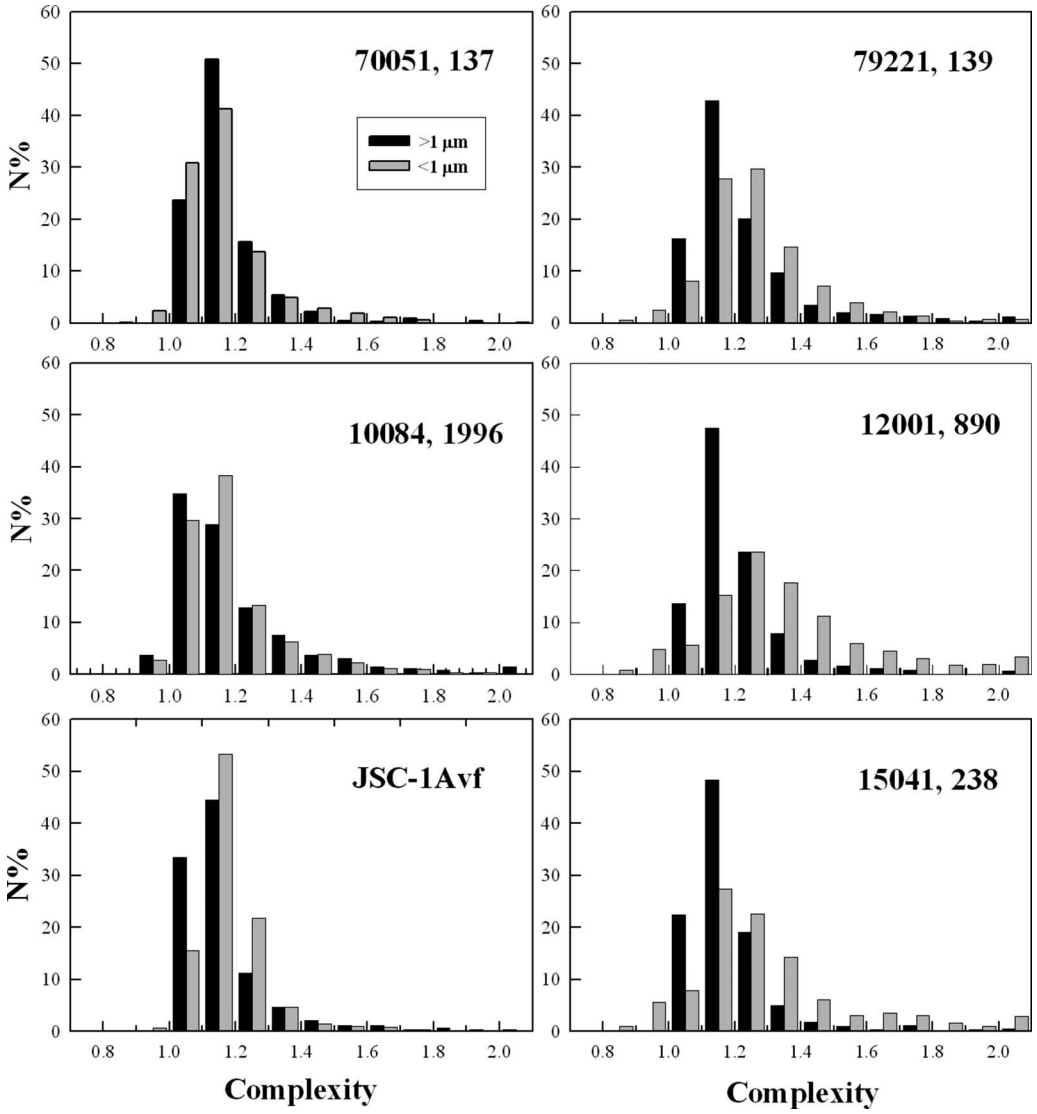

Fig. 4. Complexity of five lunar soils and a simulant JSC-1Avf

JSC-1Avf also lacks the complex surface texture (glass mounds) and the submicron vesicles. Third, JSC-1Avf does not contain any nanophase iron. This simulant with addition of another simulant that contains nanophase iron (Liu et al. 2007) may be sufficient for toxicity studies with animal subjects. Therefore, JSC-1Avf is unlikely to simulate the large reaction surface areas observed in vesicular lunar dust grains. In addition, as shown by Park et al. (2008), JSC-1Avf does not possess the proper particle-size distribution for being a good lunar dust analog, as far as particle size is concerned.

Implication on Toxicity

The composition, size, and morphology of dust particles are important for understanding their deposition and clearance mechanisms in the lung (Guthrie 1997). Deposition mechanisms include impaction, sedimentation, interception, electrostatic deposition, diffusion, and chaotic mixing (Plumlee et al. 2006, and references cited therein). Our study demonstrates that lunar dust particles have jagged edges, which may cause the "Velcro" effect of the particle with the wall of trachea, once deposited. The vesicle-bearing particles have less density and thus, can possibly be carried deeper into the lungs than equal mass particles. The toxicity of the particles is related to the speed with which they are cleared from the lung. Most of the large particles (>3 μm) deposited on trachea and primary bronchi will be trapped by mucus and cleared out by coughing. The remaining smaller particles ($<\sim 3$ μm) are mainly removed through phagocytosis by airway and alveolar macrophages through dissolution, the latter mainly for alveoli. Particles engulfed by macrophages are subjected to an acidic fluid (the lysosomal fluid) with pH=4.5 (Plumlee et al. 2006). This acidic fluid may be able to dissolve the metastable glass. The complex features (vesicles and glass mounds) of lunar dust particles increase the reaction surface area of the particle, and thus, aid the dissolution rate of dust particles. During the dissolution processes, the large number of np-Fe^0 particles embedded in the glass may affect the fluid and cell chemistry, which need to be investigated through medical tests. For smaller particles of <1 μm size, sharp edges may aid their translocation from the

Sample	Particle image	Vesicles on particle	Porosity, Area Ratio, Total number of vesicles
10084, 1998	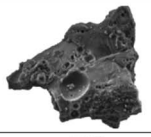	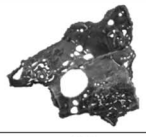	$A_v/A_t = 0.13$ $P_v/P_{sp} = 2.15$ $\Sigma N_v = 110$
10084, 1998			$A_v/A_t = 0.30$ $P_v/P_{sp} = 1.88$ $\Sigma N_v = 24$
10084, 1998	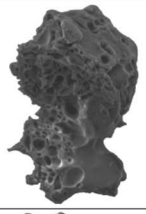		$A_v/A_t = 0.18$ $P_v/P_{sp} = 3.61$ $\Sigma N_v = 154$
70051, 137	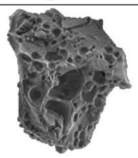	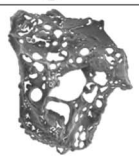	$A_v/A_t = 0.25$ $P_v/P_{sp} = 4.6$ $\Sigma N_v = 145$
70051, 137	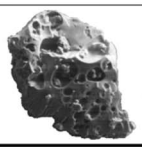	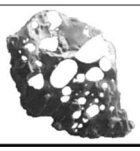	$A_v/A_t = 0.26$ $P_v/P_{sp} = 2.23$ $\Sigma N_v = 39$

Fig. 5. Surface area of vesicular lunar grains. All vesicles and particles are assumed to be half-spheres. P and A stand for perimeter and area, respectively. Subscripts v, sp, and t refer to vesicle-bearing particle, volume-equivalent solid particle, and total, respectively. ΣN_v=total number of vesicles.

alveolar region to the blood circulation. The near-neutral pH value of the blood (Plumelee et al. 2006) will make the dissolution of the dust particles more difficult. Additionally, the dissolution of dust materials or simulants with similar composition and shape needs to be studied to determine the interaction of np-Fe^0 with blood, particularly with effects on Fe^{3+} and Fe^{2+}.

Summary

The distribution of aspect ratios and complexity factors of five Apollo lunar dust samples are reported; this is the first study on the shape of submicron lunar dust particles. In general, lunar dust grains have jagged edges and rugged profiles, which can affect the deposition of particles in human lungs. Lunar dust particles commonly contain abundant nanophase metallic iron, both on the surfaces of particles and also within glass. These coatings form glass mounds, which increase the reactive surface area of the particles. There are also vesicular lunar dust particles, which contain a large reaction surface area. For such particles with increased reactive surface area, the dissolution rates of particles in fluids with different pH values, as found in human body, needs to be studied. The effects of nanophase metallic iron on cells or enzymes also need to be investigated. This present study compares Apollo dust to the simulant JSC-1Avf and provides important data necessary for studies of lunar dust toxicology.

Acknowledgments

The writers would like to thank three anonymous reviewers for their constructive comments. They also thank Yinghong Liu and Gregory Jones for their assistance with the SEM instruments, and Dr. David Joy for the access to his electron microscopy laboratories. This work is partially supported by a NASA contract from JSC for dust mitigation studies, for which we are grateful. Additional funding was provided by the Planetary Geosciences Institute.

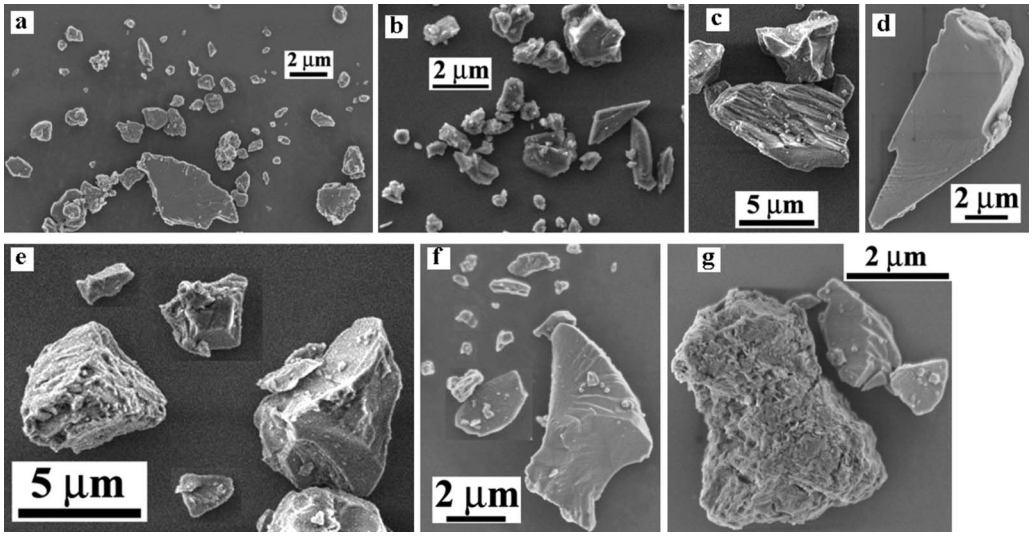

Fig. 6. SEM images of lunar dust simulant JSC-1Avf. All samples were cleaned with the surfactant solution.

References

Alshibli, K. A., and Alsaleh, M. I. (2004). "Characterizing surface roughness and shape of sands using digital microscopy." *J. Comput. Civ. Eng.*, 18(1), 36–45.

Barrett, P. J. (1980). "The shape of rock particles: A critical review." *Sedimentology*, 27(3), 291–303.

Bouwman, A. M., Bosma, J. C., Vonk, P., Wesselingh, J. A., and Frijlink, H. W. (2004). "Which shape factor(s) best describe granules?" *Powder Technol.*, 146(1–2), 66–72.

Carter, J. L., and MacGregor, I. D. (1970). "Mineralogy, petrology and surface features of some Apollo 11 samples." *Proc., Apollo 11 Lunar Sci. Conf.*, Vol. 1, Pergamon Press, Inc., New York, 247–265.

Cloud, P., et al. (1970). "Micromorphology and surface characteristics of lunar dust and breccia." *Proc., Apollo 11 Lunar Sci. Conf.*, Vol. 1, Pergamon Press, Inc., New York, 1793–1798.

Darquenne, C., Paiva, M., West, J. B., and Prisk, G. K. (1997). "Effect of microgravity and hypergravity on deposition of 0.5- to 3-μm-diameter aerosol in the human lung." *J. Appl. Physiol.*, 83(6), 2029–2036.

Darquenne, C., West, J. B., and Prisk, G. K. (1998). "Deposition and dispersion of 1 μm aerosol boluses in the human lung: Effect of micro- and hypergravity." *J. Appl. Physiol.*, 85(4), 1252–1259.

Darquenne, C., West, J. B., and Prisk, G. K. (1999). "Dispersion of 0.5–2 μm aerosol in micro- and hypergravity as a probe of convective inhomogeneity in the human lung." *J. Appl. Physiol.*, 86(4), 1402–1409.

Delfino, R. J., Sioutas, C., and Malik, S. (2005). "Potential role of ultrafine particles in associations between airborne particle mass and cardiovascular health." *Environ. Health Perspect.*, 113(8), 934–946.

Fruland, R. M., Morris, R. V., McKay, D. S., and Clanton, U. S. (1977). "Apollo 17 ropy glasses." *Proc., 8th Lunar Sci. Conf.*, Vol. 3, Pergamon Press, Inc., New York, 3095–3111.

Fulchignoni, M., Funiciello, R., Taddcucci, A., and Trigila, R. (1971). "Glassy spheroids in lunar fines from Apollo 12 samples 12070,37; 12001,73; and 12057,60." *Proc., 2nd Lunar Sci. Conf.*, Vol. 2, The M.I.T. Press, Cambridge, Mass., 937–848.

Görz, H., White, E. W., Johnson, G. G., Jr., and Pearson, M. W. (1972). "CESEMI studies of Apollo 14 and 15 fines." *Proc., 3rd Lunar Sci. Conf.*, Vol. 2, The M.I.T. Press, Cambridge, Mass., 3195–3200.

Görz, H., White, E. W., Roy, R., and Johnson, G. G., Jr. (1971). "Particle size and shape distributions of lunar fines by CESEMI." *Proc., 2nd Lunar Sci. Conf.*, Vol. 2, The M.I.T. Press, Cambridge, Mass., 2021–2025.

Guthrie, G. D., Jr. (1997). "Mineral properties and their contribution to particle toxicity." *Environ. Health Perspect.*, 105, 1003–1011.

Gwinn, M. R., and Vallyathan, V. (2006). "Nanoparticles: Health effects—Pros and cons." *Environ. Health Perspect.*, 114(12), 1818–1825.

Heywood, H. (1971). "Particle size and shape distribution for lunar fines sample 12057,72." *Proc. Lunar Sci. Conf., 2nd*, Vol. 2, The M.I.T. Press, Cambridge, Mass., 1989–2001.

Hill, E., Mellin, M. J., Deane, B., Liu, Y., and Taylor, L. A. (2007). "Apollo sample 70051 and high- and low-Ti lunar soil simulants MLS-1A and JSC-1A: Implications for future lunar exploration." *J. Geophys. Res.*, 112(E2), E02006.

Holland, J. W., and Simmonds, R. C. (1973). "The mammalian response to lunar particulates." *Space Life Sci.*, 4(1), 97–109.

James, J. T. (2005). "Mammalian toxicity of lunar dust and related simulants." *Biological Effects of Lunar Dust Workshop*, ⟨http://lstworkshop.arc.nasa.gov/⟩ (last accessed October 2006).

Keller, L. P., and McKay, D. S. (1993). "Discovery of vapor deposits in the lunar regolith." *Science*, 261(5126), 1305–1307.

Keller, L. P., and McKay, D. S. (1997). "The nature and origin of rims on lunar soil grains." *Geochim. Cosmochim. Acta*, 61(11), 2331–2341.

Klosky, J. L., Sture, S., Ko, H. Y., and Barnes, F. (1996). "Mechanical properties of JSC-1 lunar regolith simulant." *Space V*, ASCE, Reston, Va., 680–688.

Kustov, V. V., Belkin, V. I., and Kruglikov, G. G. (1989). "Biological effects of lunar soil." *Probl in Space Biol.*, 61, 146.

Lam, C. W., James, J. T., Latch, J. N., Hamilton, R. F., and Holian, A. (2002a). "Pulmonary toxicity of simulated lunar and MArtian dusts in mice: II. Biomarkers of acute responses after intratracheal instillation." *Inhalation Toxicol.*, 14(9), 917–928.

Lam, C. W., James, J. T., McCluskey, R., Cowper, S., Balis, J., and Muro-Cacho, C. (2002b). "Pulmonary toxicity of simulated lunar and MArtian dusts in mice: I. Histopathology 7 and 90 days after intratracheal instillation." *Inhalation Toxicol.*, 14(9), 901–916.

Liu, Y., Park, J. S., Hill, E., Kihm, K. D., and Taylor, L. A. (2006). "Morphology and physical characteristics of Apollo 17 dust particles." *10th ASCE Aerospace Division Int. Conf.* (CD-ROM), Houston.

Liu, Y., Taylor, L. A., Thompson, J. R., Schnare, D., and Park, J. S. (2007). "Unique properties of lunar impact glass: Nanophase metallic Fe synthesis." *Am. Mineral.*, 92(8–9), 1420–1427.

McKay, D. S., et al. (1991). "The lunar regolith." *Lunar sourcebook*, G. Heiken, D. Vaniman, and B. French, eds., Cambridge University Press, New York, 286–356.

McKay, D. S., Carter, J. L., Boles, W. W., Allen, C. C., and Allton, J. H. (1994). "JSC-1: A new lunar soil simulant." *Proc., Space '94*, ASCE, New York, 857–866.

McKay, D. S., Clanton, U. S., and Ladle, G. (1973). "Scanning electron microscope study of Apollo 15 green glass." *Proc., 4th Lunar Sci. Conf.*, Vol. 1, Pergamon Press, Inc., New York, 225–238.

McKay, D. S., Greenwood, W. R., and Morrison, D. A. (1970). "Origin of small lunar particles and breccia from the Apollo 11 site." *Proc., Apollo 11 Lunar Sci. Conf.*, Vol. 1, Pergamon Press, Inc., New York, 673–694.

Mills, N. L., et al. (2006). "Do inhaled carbon nanoparticles translocate directly into the circulation in humans?" *Am. J. Respir. Crit. Care Med.*, 173(4), 426–431.

Mueller, G. (1971). "Morphology and petrostatistics of regular particles in Apollo 11 and Apollo 12 fines." *Proc., 2nd Lunar Sci. Conf.*, Vol. 3, The M.I.T. Press, Cambridge, Mass., 2041–2047.

Nemmar, A., Hoct, P. H. M., Vanquickenborne, B., Dinsdale, D., Thomeer, M., Hoylaerts, M. F., Vanbillocn, H., Mortlmans, L., and Nemery, B., (2002). "Passage of inhaled particles into the blood circulation in humans." *Circulation*, 105(4), 411–414.

Noble, S., Pieters, C. M., Taylor, L. A., Morris, R. V., Allen, C. C., McKay, D. S., and Keller, L. P., (2001). "The optical properties of the finest fraction of lunar soil: Implications for space weathering." *Meteorit. Planet. Sci.*, 36(1), 31–42.

Park, J. S., Liu, Y., Kihm, K. D., Greenberg, P., and Taylor, L. A. (2008). "Characterization of lunar dust for toxicological studies. I: Particle size distribution." *J. Aerosp. Eng.*, 21(4), 272–279.

Park, J. S., Liu, Y., Kihm, K. D., Hill, E., and Taylor, L. A. (2006a). "Submicron particle size distribution of Apollo 11 lunar dust." *10th ASCE Aerospace Division International Conf.* (CD-ROM), Houston.

Park, J. S., Liu, Y., Kihm, K. D., and Taylor L. A., (2006b). "Toxicity of lunar dust for humans at a lunar base." *S. E. Section Geol. Soc. Amer, Conf., Abstract* (CD-ROM), 102500.

Plumlee, G. S., Morman, S. A., and Ziegler, T. L. (2006). "The toxicological geochemistry of earth materials: An overview of processes and the interdisciplinary methods used to understand them." *Rev. Mineral. Geochim.*, 64, 5–57.

Taylor, L. A., Pieters, C. M., Keller, L. P., Morris, R. V., and McKay, D. S. (2001). "Lunar mare soils: Space weathering and the major effects of surface-correlated nanophase Fe." *J. Geophys. Res.*, 106(E11), 27985–27999.

Taylor, L. A., Schmitt, H. H., Carrier, W. D., and Nakagawa, M. (2005). "The lunar dust problem: From liability to asset." *1st Space Explor. Conf.*, AIAA, Orlando, Fla.

Wentworth, S. J., Keller, L. P., McKay, D. S., and Morris, R. V. (1999). "Space weathering on the Moon: Patina on Apollo 17 samples 75075 and 76015." *Meteorit. Planet. Sci.*, 34(4), 593–603.